Available online at www.sciencedirect.com
ScienceDirect
Trans. Nonferrous Met. Soc. China 21(2011) 974−984
Transactions of Nonferrous Metals Society of China
www.tnmsc.cn

Effect of axial force on microstructure and tensile properties of friction stir welded AZ61A magnesium alloy

A. RAZAL ROSE[1], K. MANISEKAR[2], V. BALASUBRAMANIAN[3]

1. Department of Mechanical Engineering, National Engineering College, K.R. Nagar−628502, Kovilpatti, Tamil Nadu, India;
2. Centre for Manufacturing Sciences, Department of Mechanical Engineering, National Engineering College, K.R Nagar−628502, Kovilpatti, Tamil Nadu, India;
3. Department of Manufacturing Engineering, Annamalai University, Annamalainagar−608002, Chidambaram, Tamil Nadu, India

Received 22 July 2010; accepted 3 December 2010

Abstract: The influences of axial force on tensile properties of friction stir welded AZ61A magnesium alloy were studied. Five different values of axial forces ranging from 3 to 7 kN were used to fabricate the joints. Tensile properties of the joints were evaluated and correlated with the stir zone microstructure and hardness. From this investigation, it is found that the joint fabricated with an axial force of 5 kN exhibits superior tensile properties compared to other joints. The formation of finer grains in the stir zone and higher hardness of the stir zone are the main reasons for the superior tensile properties of these joints.
Key words: AZ61A magnesium alloy; friction stir welding; tensile properties; microhardness; microstructure

1 Introduction

Structural applications of magnesium alloys are rapidly increasing in automotive and aerospace equipment due to their low density and high specific strength[1]. In the automotive and aerospace industries, the need to reduce fuel consumption and associated costs has led to the replacement of heavy components with lighter alloys. Moreover, magnesium alloys are 35% lighter than aluminium and possess good machining and casting characteristics. Furthermore, they have excellent specific strength, high elastic modulus and good vibration/damping properties[2]. They are also considered advanced materials in terms of energy conservation and environmental pollution regulations. However, the joining of magnesium alloy parts which may be crucial for the above applications is still limited[3].

Fusion welding of magnesium alloys produces some defects such as porosity and hot crack, which deteriorates their mechanical properties. The production of the defect-free weld requires complete elimination of the surface oxide layer and selection of suitable welding parameters. Although reasonable welding speed can be achieved, some problems are aroused such as high-welding residual stresses and changes in microstructure resulting from melting and solidification. High-purity shielding gases are necessary to prevent weld contamination; magnesium alloys can readily oxidize in the weld zone because of their high-chemical reactivity at high temperatures[4]. Friction stir welding (FSW) is capable of joining magnesium alloys without melting and thus it can eliminate problems related to the solidification. As FSW does not require any filler material, the metallurgical problems associated with it can be also reduced and good quality weld can be obtained[5].

Even though the process offers many advantages, very limited investigations have been carried out so far on FSW of magnesium alloys. The relationship between material flow and defects formation during friction stir welding of AZ31 magnesium alloy was reported by ZHANG et al[6]. Grain growth and lower hardness in the FSW zone of AZ31B-H24 magnesium alloy were reported by LEE et al[7]. WANG et al[8] observed grain refinement and higher micro hardness in FSW zone of AZ31 magnesium alloy. PAREEK et al[9] investigated

Corresponding author: A. RAZAL ROSE; Tel: +91-09487897397; +91-462-2551360; Fax: +91-4144-238080/238275; E-mail: razalrose2007@rediffmail.com
DOI: 10.1016/S1003-6326(11)60809-1

the microstructural changes due to friction stir welding of AZ31B-H24 magnesium alloy and analysed their effect on mechanical properties and corrosion behaviour of the joints. They found that the mean grain size across all weld samples was coarser than that of the as-received magnesium alloy samples. The influence of different ratios of rotational speed/traverse speed on mechanical properties of different zones of friction stir welded AZ31 magnesium alloy was studied by ABBASI GHARACHEH et al[10]. ESPARZA et al[11] found a recrystallized and equiaxed grain structure in the FSW zone of AZ31B magnesium alloy. The effect of welding speed on the material flow patterns was studied by ZHANG et al[12]. They suggested that there were two main material flows in the nugget, one was from the advancing side (flow 1), the other was from the retreating side (flow 2), and flow 2 decided whether the weld was defect-free or not. CAO et al[13] investigated the influence of welding speed on the joint quality of friction stir welded AZ31B-H24 magnesium alloy. They concluded that the hardness decreased gradually from the base metal through the heat-affected zone to the thermo mechanically affected zone and then to the stir zone where the lowest hardness was obtained. Higher welding speed produced slightly higher hardness in the stir zone.

KAZUHIRO et al[14] investigated the effect of tool rotational speed and welding speed on the formation of defect in various grades of magnesium alloys. They reported that magnesium alloys with higher aluminium contents were difficult to join without defects and the optimum welding parameters were restricted to narrow region. PARK et al[15] attempted to relate the microstructural and mechanical properties of friction stir welded AZ61 grade magnesium alloy. They found that the tensile properties of AZ61 grade magnesium alloy were sharply influenced by crystallographic orientation distribution as well as by grain size and dislocation density. DU and WU[16] used friction stir processing technique combined with rapid heat sink to produce ultra-fine grained structure in AZ61 magnesium alloy. It was observed that the hardness of FSP region was five times higher than that of base metal and the grain size was reduced to 300 nm. SRINIVASAN et al[17] investigated the stress corrosion cracking behaviour of friction stir welded AZ61 grade wrought magnesium alloy. They found that the weld nugget region was quite susceptible to stress corrosion cracking even at a strain rate of 10^{-6} s^{-1}. However, in electrochemical test the weld nugget showed a better corrosion resistance than the base metal.

From above, it is understood that the published information on friction stir welding of magnesium alloys is less in number compared to aluminium alloys. Further, most of the investigations on magnesium alloys were carried out on AZ31 alloy[4−13] which contains 3% aluminium and 1% zinc. Recently, a few studies[14−17] have been carried out to evaluate the weld ability of AZ61 grade magnesium alloys. However, the effect of FSW process parameters on mechanical and metallurgical properties of AZ61A grade magnesium alloy has not yet been understood clearly as AZ31 grade magnesium alloy. Moreover, most of the reports available in open literature have focused on the effect of tool rotational speed and welding speed. KRISHNAN et al[18] studied the mechanism of onion ring formation in the friction stir welds of aluminium alloys. They found that the material flow patterns highly depended upon the axial force. They also opined that at low axial force, the formation of nonsymmetrical semi-circular features at the top surface of the weld showed poor plasticization. Due to higher axial force, the formation of shear lips or flashes with excessive height on both advancing and retreating sides of the weld line resulted in excessive thinning of the metal in the weld area yielding poor tensile properties. OUYANG et al[19] reported that in friction stir welded AA6061 alloy, the shoulder force that was directly responsible for the plunge depth of the tool pin into the surface of the work piece was very changeable during the plungement. The material flow patterns highly depended upon the geometry of the threaded tool, welding temperature, material flow stress and axial force. BUFFA et al[20] proved that the heat generation in FSW AA7075 alloy was in direct proportion to deformation and frictional energy generated in the welding. The latter depended on the friction coefficient and friction area between the tool shoulder and work piece surface as well on the rotation speed of the welding head pin and the pressure applied to the welding head shoulder. KUMAR et al[21] investigated the influence of axial load and the effect of position of the interface with respect to the tool axis on tensile strength of the friction stir welded AA7020 T6 joint. The fracture occurred in the weld nugget region in tensile samples taken from the weld under axial load from 4.0 to 6.7 kN, while fracture occurred away from the weld nugget in samples taken from the weld under axial load higher than 7.4 kN. It could also be seen that the tensile strength was lower and more or less constant when the axial loads were less than 6.0 kN. When the axial load increased from 6.0 to 7.4 kN, the tensile strength increased suddenly and was more or less constant above 7.4 kN. ELANGOVAN et al[22] reported the effect of axial force on tensile properties of friction stir welded AA6061 aluminium alloy. The joint fabricated under 6 kN axial force consisted of coarse grains with bundle of strengthening precipitates (black particles). Similarly, the joint fabricated at 8 kN axial force consisted of coarse grains but the strengthening precipitates became very fine and uniformly distributed throughout the matrix due to excessive axial force. The joint fabricated with 7 kN axial force consisted of fine, equiaxed grains with uniform distribution of fine strengthening precipitates throughout the matrix. JAYARAMAN et al[23] studied the effect of four axial force levels on the fabrication of the aluminium alloy joints. The joint fabricated under an axial force of 2 kN exhibited tunnel defect at the middle of the weld zone due to insufficient material flow, but the joint fabricated under 4 kN axial force resulted in nonuniform distribution of Si particles and thinning of weld nugget due to the excess axial force. The joint fabricated under 3 kN axial force consisted of fine, eutectic Si particles with uniform distribution throughout the aluminium matrix due to the sufficient flow of softened material. This may be the reason for higher tensile strength of the joints fabricated under 3 kN axial force compared to their counterparts. PADMANABAN et al[24] studied the effect of axial force on tensile strength of friction stir welded AZ31B magnesium alloy joints. When the axial force was relatively low, there was a possibility of insufficient stirring (less mechanical working) at the bottom. While with higher axial force, the weld was sound with full penetration. It showed that sufficient axial force was required to form good weld because the temperature during friction stir welding defined the amount of plasticized metal but the temperature was greatly dependent on the axial force.

The researches on the effect of axial force on FSW joint properties of AZ61A magnesium alloy were relatively few. Hence, in this investigation, an attempt was made to study the effect of axial force on the tensile properties of FSW joints of AZ61A magnesium alloy.

2 Experimental

The extruded plates of 6 mm thick AZ61A grade magnesium alloy were used in this investigation. The chemical composition and mechanical properties of the base metal are presented in Tables 1 and 2, respectively. The optical micrograph of base metal is shown in Fig.1. Square butt joint configuration with size of 300 mm×300 mm was used to fabricate the joints. The initial joint configuration was obtained by securing the plates in position using mechanical clamps. The direction of welding was normal to the extrusion direction. Non-consumable tool made of high carbon steel (as shown in Fig.2) was used to fabricate the joints. The dimensions of the tool are presented in Table 3. Single pass welding procedure was followed to fabricate the joints. Computer controlled FSW machine (R.V. Machine Tools, India; capacity: 60 kN; 3 000 r/min) was used to fabricate the joints. Five joints were fabricated in this investigation under five levels of axial force, and other parameters were constant. The parameters used to fabricate the joints during FSW process are presented in Table 4.

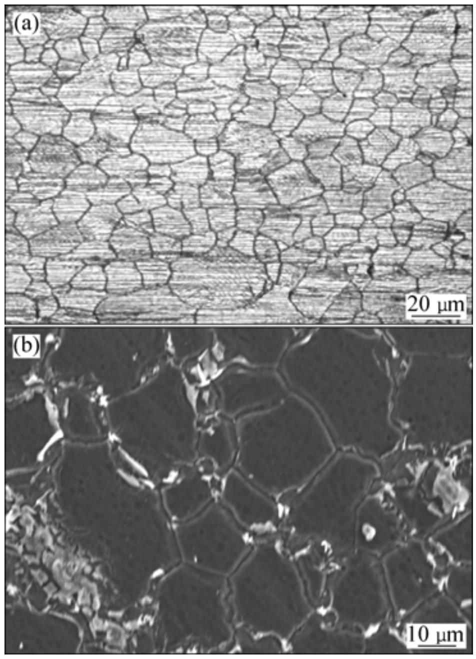

Fig.1 Optical (a) and SEM (b) images of base metal

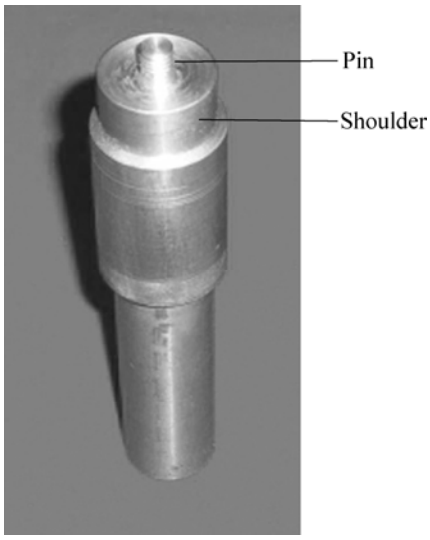

Fig.2 Photograph of tool used to fabricate joints

Table 1 Chemical composition of base metal (mass fraction, %)

Al	Mn	Zn	Mg
5.96	0.17	1.28	Bal.

Table 2 Mechanical properties of base metal

Yield strength/ MPa	Ultimate tensile Strength/ MPa	Elongation/ %	Reduction in cross-sectional area/%	Hardness (HV)
217	271	8.40	14.3	70.0

Table 3 Parameters of FSW tool

Parameter	Value
Tool shoulder diameter, D/mm	18
Tool pin diameter, d/mm	6
D/d ratio of tool	3.0
Pin length, L/mm	5.9
Tool inclined angle/(°)	0
Shoulder depth inserted into surface of base metal/mm	0.1
Tool pin profile	Threaded
Pitch of threaded pin/mm	1
Included angle of threaded pin	60
Tool material	High carbon steel (HCS)
Tool material composition	0.75% C, 0.25% Si, 0.32% Mn and balance Fe

Table 4 Parameters of FSW process

Joint number	Tool rotational speed/(r·min^{-1})	Welding speed/ (mm·min^{-1})	Axial force/kN	Heat input*/ (J·mm^{-1})
1	1200	90	3	181
2	1200	90	4	242
3	1200	90	5	302
4	1200	90	6	362
5	1200	90	7	422

* The heat input for friction stir welding process is calculated using the following expression [26] $q=2\pi/3S\mu P\omega R_s\eta$, where μ is the coefficient of friction; P is the normal force in kN; ω is the rotational speed in r/s; R_s is the shoulder radius in m; S is the welding speed in mm/min; η is the efficiency of the process (assumed as 0.8).

From each joint, three tensile specimens were extracted from the mid-length of the joint and ASTM E8M-04 guide lines for sheet type material with dimensions of 50 mm×12.5 mm×200 mm were followed to prepare the specimen. The dimensions of tensile specimen are shown in Fig.3(a). Figure 3(b) displays the joints and tensile specimens prepared in this investigation. Smooth tensile specimens were prepared to evaluate the yield strength, tensile strength, elongation and joint efficiency. Notch tensile specimens were prepared to evaluate the notch tensile strength and notch strength ratio, the dimensions of which are shown in Fig.3(c). Tensile test was carried out under a load of 100 kN on an electro-mechanically controlled universal testing machine (FIE-Bluestar, India; UNITEK-94100). The 0.2% offset yield strength and the elongation were recorded. Vicker's microhardness testing machine (SHIMADZU, Japan; HMV-2T) was employed to measure the hardness across the weld region under 0.49 N load for 20 s. The specimens for metallographic examination were sectioned to the required dimensions and then polished using different grades of emery papers. Polished samples were etched with an acetopicral solution of 0.4 g picric acid, 13 mL ethanol, 3 mL glacier acetic acid and 3 mL boiled water to reveal the microstructure of the welded joints. Macro and micro structural analyses were carried out using a light optical microscope (MEIJI, Japan; MIL-7100) incorporated with an image analyzing software (Metal Vision). Fracture surface of the tensile specimens were analysed by scanning electron microscopy (JOEL, Japan; 5610 LV) to reveal the mode of fracture.

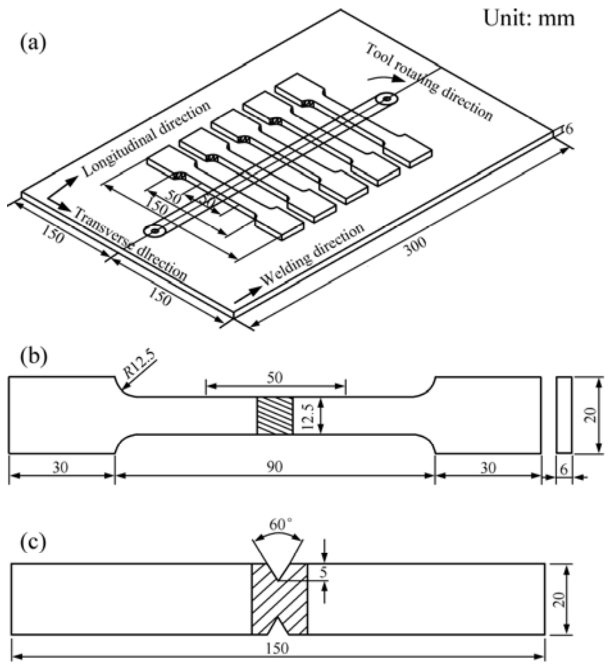

Fig.3 Configuration of joint and tensile specimen: (a) Scheme of extraction of tensile specimen; (b) Dimensions of flat tensile specimen; (c) Dimensions of notched tensile specimen (unit: mm)

3 Results

3.1 Tensile properties

The transverse tensile properties such as yield strength, tensile strength, notch tensile strength, notch strength ratio, elongation, reduction in cross-sectional area and joint efficiency of friction stir welded AZ61A magnesium alloy joints were evaluated. Under each condition, three specimens were tested and the average of three results is presented in Table 5. It can be inferred that the axial force has an appreciable influence on the tensile properties of welded joints. The strain—stress curves of base metal and welded joints are displayed in Fig.4. The yield strength and tensile strength of base metal are 217 and 271 MPa, respectively. Among the five joints, the joint fabricated under the condition of axial force of 5 kN, tool rotational speed of 1 200 r/min, welding speed of 90 mm/min and heat input of 302 J/mm exhibits higher yield strength of 177 MPa, tensile strength of 224 MPa, elongation of 7.2% and joint efficiency of 83%. Notch strength ratio (NSR) is found to be less than the unity irrespective of the welded joints. This suggests that AZ61A magnesium alloy is sensitive to notches, which falls in the notch brittle materials category. The NSR is 0.92 for the unwelded parent metal and FSW causes reduction in NSR of the weld metal. Table 5 lists the tensile properties of joints fabricated under different axial forces. It can be seen that the joints fabricated using axial force of 3 kN (heat input of 181 J/mm) show lower tensile strength and elongation compared to the joints fabricated under axial force of 5 kN. Similarly, the joints fabricated under axial force of 7 kN (heat input of 422 J/mm) also show lower tensile strength and elongation compared to the joint fabricated at axial force of 5 kN. To understand the reason for variation in tensile properties of the joints, macrostructure analysis, microstructure analysis and micro hardness measurements were carried out and the results are presented in the following sections.

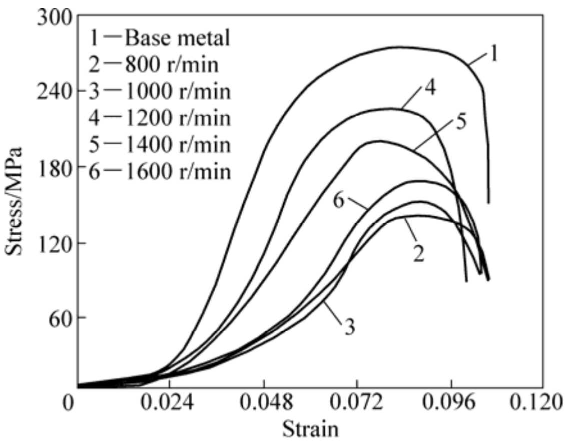

Fig.4 Stress—strain curves of joints welded at different rates

3.2 Macrostructure

In fusion welding of magnesium alloys, defects like porosity, slag inclusion and solidification cracks, etc. deteriorate the weld quality and joint properties. Usually, friction stir welded joints are free from these defects since there is no melting taking place during welding and the metals are joined in the solid state itself due to the heat generated by the friction and metal flow caused by the stirring action. However, FSW joints are prone to other defects like pinhole, tunnel defect, piping defect, kissing bond and cracks, etc due to improper flow of metal and insufficient consolidation of metal in the stir zone (SZ). The weld cross section of the joints was analyzed at low magnification using stereo zoom optical microscope and the macrographs are shown in Fig.5. From the macrographs, features like SZ shape, SZ dimension (height and width) and presence of defects were analysed and they are listed in Table 6. From the macrostructure analysis, it can be inferred that the formation of defect free FSW welds is a function of optimum axial force (heat input). From the macrostructure analysis, it is found that the joint fabricated at an axial force of 5 kN yielded spherical shaped and defect free stir zone, which may be one of the reasons for superior tensile properties of these joints.

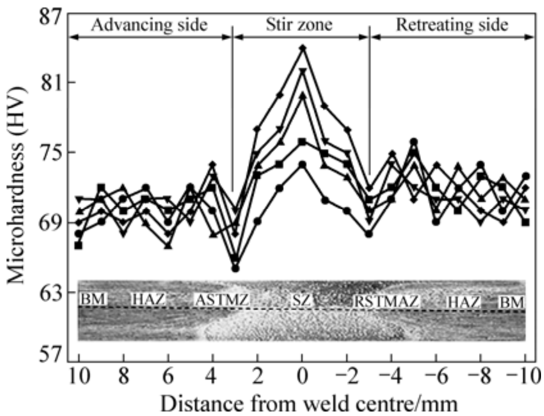

Fig.5 Hardness and macrographs of different parts in joints

3.3 Microhardness

Microhardness was measured at mid thickness region across the weld and the values are presented in Fig.5. The base metal recorded a hardness of HV 70, which is lower than that of stir zone but higher than that of thermo mechanically affected zone (TMAZ) region. The hardness of the stir zone is considerably higher than that of the base metal irrespective of the welding speed used. There are two main reasons for the improved hardness of stir zone. 1) The grain size of stir zone is

Table 5 Tensile properties of joints fabricated under different axial forces

Axial force/kN	Yield strength/MPa	Ultimate tensile strength/MPa	Notch tensile strength/MPa	Notch strength ratio	Elongation in 50 mm gauge length/%	Reduction in cross-sectional area/%	Joint efficiency/%
3	137	171	130	0.76	4.1	3.2	63.0
4	151	189	148	0.79	5.4	3.9	70.0
5	177	224	190	0.85	7.2	5.1	83.0
6	124	153	118	0.77	5.1	3.6	57.0
7	110	138	104	0.75	3.4	2.8	51.0

Table 6 Macrostructure analysis of joints under different axial forces

Axial force/kN	Macrostructure		Size of stir zone/mm		Shape of stir zone	Name of defect and location	Quality of weld metal consolidation	Probable reason
	Retreating side	Advancing side	*W*	*H*				
3	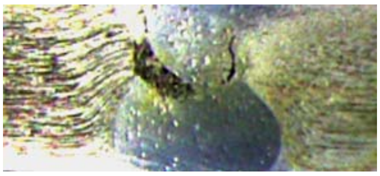		4.3 4.9 6.1	5.9	Inverted trapezoidal	Pin hole at middle of the weld on advancing side	Poor	Insufficient heat due to low axial force
4	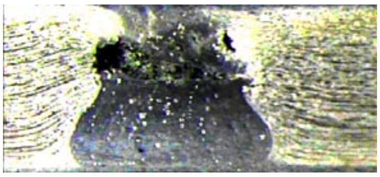		4.6 6.2 6.8	5.9	Inverted trapezoidal	Pin hole at middle of weld cross section on advancing side	Poor	Insufficient heat and no vertical flow of plasticized metal
5			6.4 5.6 6.3	5.9	Spherical	No defect	Good	Adequate heat generation and flow of material by threads
6	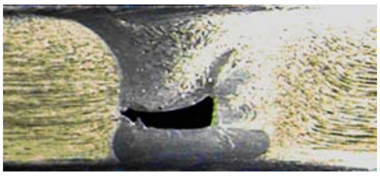		7.6 5.7 5.8	5.8	Inverted trapezoidal	Tunnel defect in bottom portion of weld on advancing side	Poor	Excess upward flow of the plasticized metal caused by threads due to additional axial force
7	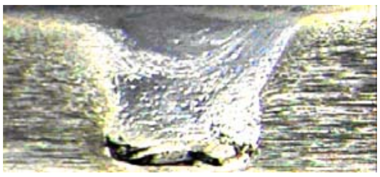		8.4 6.3 6.1	5.8	Inverted trapezoidal	Tunnel defect in bottom portion of weld on advancing side	Poor	Additional axial force leads to excess heat input and thinning of weld zone

W represents the width of SZ at top, middle and bottom, respectively; *H* represents the height of SZ

much finer than that of base metal, grain refinement plays an important role in material strengthening. According to the Hall–Petch equation, hardness increases as the grain size decreases. 2) The small particles of intermetallic compounds are also beneficial to hardness improvement, according to the Orowan hardening mechanism[8]. The difference in hardness between the heat affected zone and stir zone is attributed to the grain refinement in the stir zone. The lowest hardness was recorded in the joint fabricated with axial force of 7 kN at the TMAZ region of advancing side. The joint fabricated under axial force of 5 kN recorded the highest hardness value of HV 84 in the stir zone region and this may be one of the reasons for superior tensile properties of this joint.

3.4 Microstructure

The optical micrographs taken at stir zones of all the joints are shown in Fig.6. From the micrographs, it is understood that there is an appreciable variation in average grain diameter of the stir zone microstructure. The coarse grains of base metal are changed into fine grains in the stir zone. Hence, an attempt was made to measure the average grain diameter of the stir zone of all the joints by applying HEYN's[25] line intercept method. The joint fabricated under an axial force of 5 kN contains finer grains (12.0 μm) in the stir zone compared to other joints. This may be one of the reasons for superior tensile properties of these joints.

Optical micrographs were taken at different regions across the weld but for the comparison purpose, the micrographs of SZ/TMAZ interface regions in advancing side (AS) and retreating side (RS) are shown in Fig.7. There is an appreciable variation in grain size of TMAZ of AS and RS. The metal pulled (extruded) from AS undergoes dynamic recrystallization (characteristic

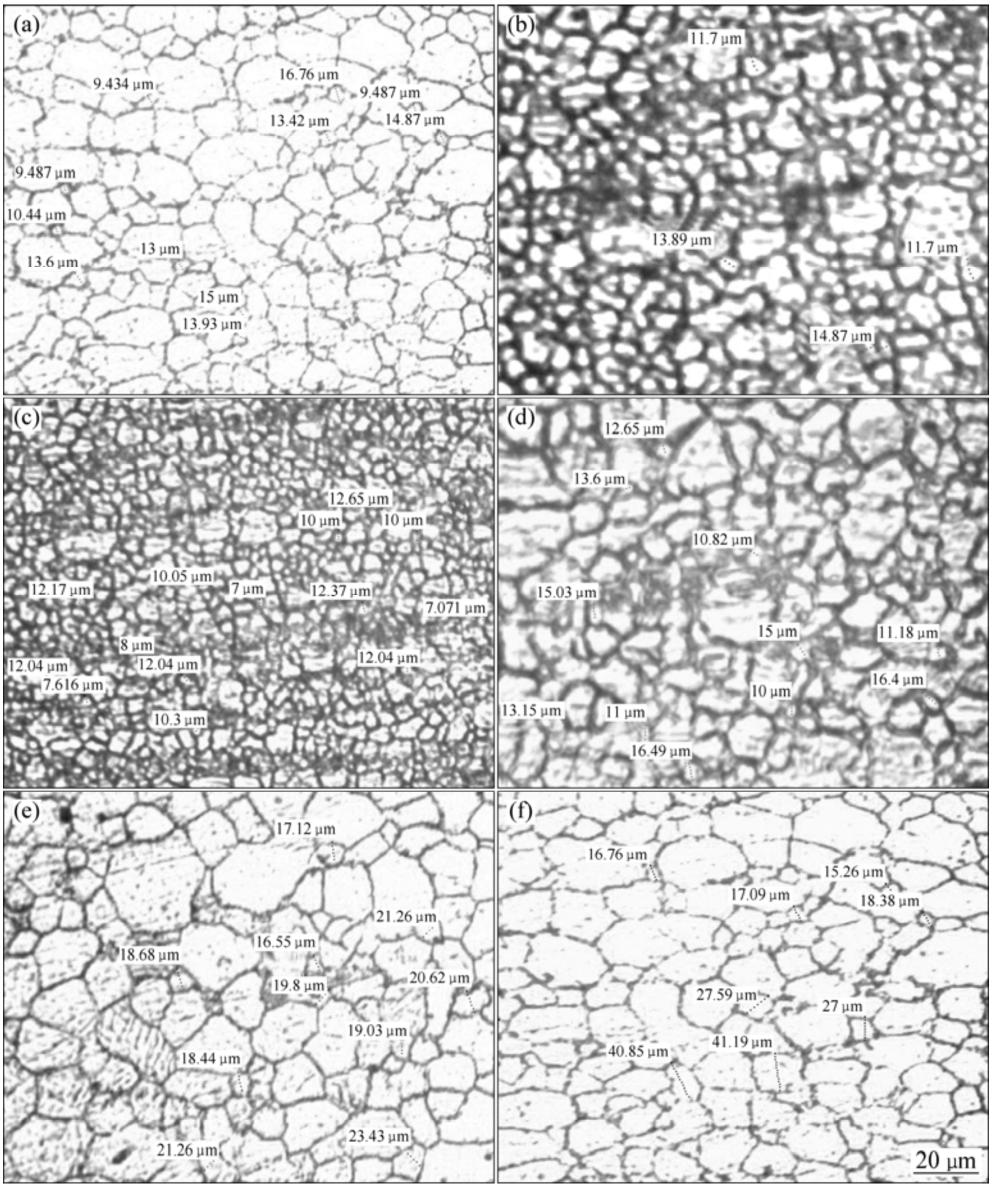

Fig.6 Stir zone microstructure under different axial force and with different average grain size: (a) 3 kN, 14.37 μm; (b) 4 kN, 13.09 μm; (c) 5 kN, 12.43 μm; (d) 6 kN, 16.8 μm; (e) 7 kN, 18.2 μm; (f) 8 kN, 42.0 μm

feature of FSW process) and redeposits on the retreating side and hence the grains are relatively finer in RSTMAZ compared to those in ASTMAZ.

The grains in the stir zone are finer than those in TMAZ. The average grain diameter of TMAZ region is influenced significantly by the welding speed. The grains are relatively finer at TMAZ of the joint fabricated under axial force of 5 kN (Fig.7(c)). However, the grains are relatively larger at the TMAZ of the joints fabricated under axial force of 6 kN (Fig.7(d)) and 7 kN (Fig.7(e)). From the micrographs, it is confirmed that the metal is extruded (pulled) from AS during stirring action of rotating tool. Due to this extrusion action, grains become elongated in TMAZ compared to base metal. Of the five joints, the joint fabricated under axial force of 5 kN contains finer grains in RSTMAZ (Fig.7(c)) compared to those in other joints. Figure 8 shows the optical micrographs of defect free joints. The optical micrographs taken at different regions of the defect free joints fabricated at an axial force of 5 kN are shown in Fig. 8. It can be seen that there is an appreciable variation in the average grain size and the coarse grains of base metal are changed into fine grains in the stir zone due to dynamic recrystallization.

3.5 Fracture surface analysis

Figure 9 shows the SEM fractographs of unnotched tensile specimens. All the fractographs invariably contain dimples and hence it is confirmed that all the joints fail in ductile mode, irrespective of the axial force (heat input)

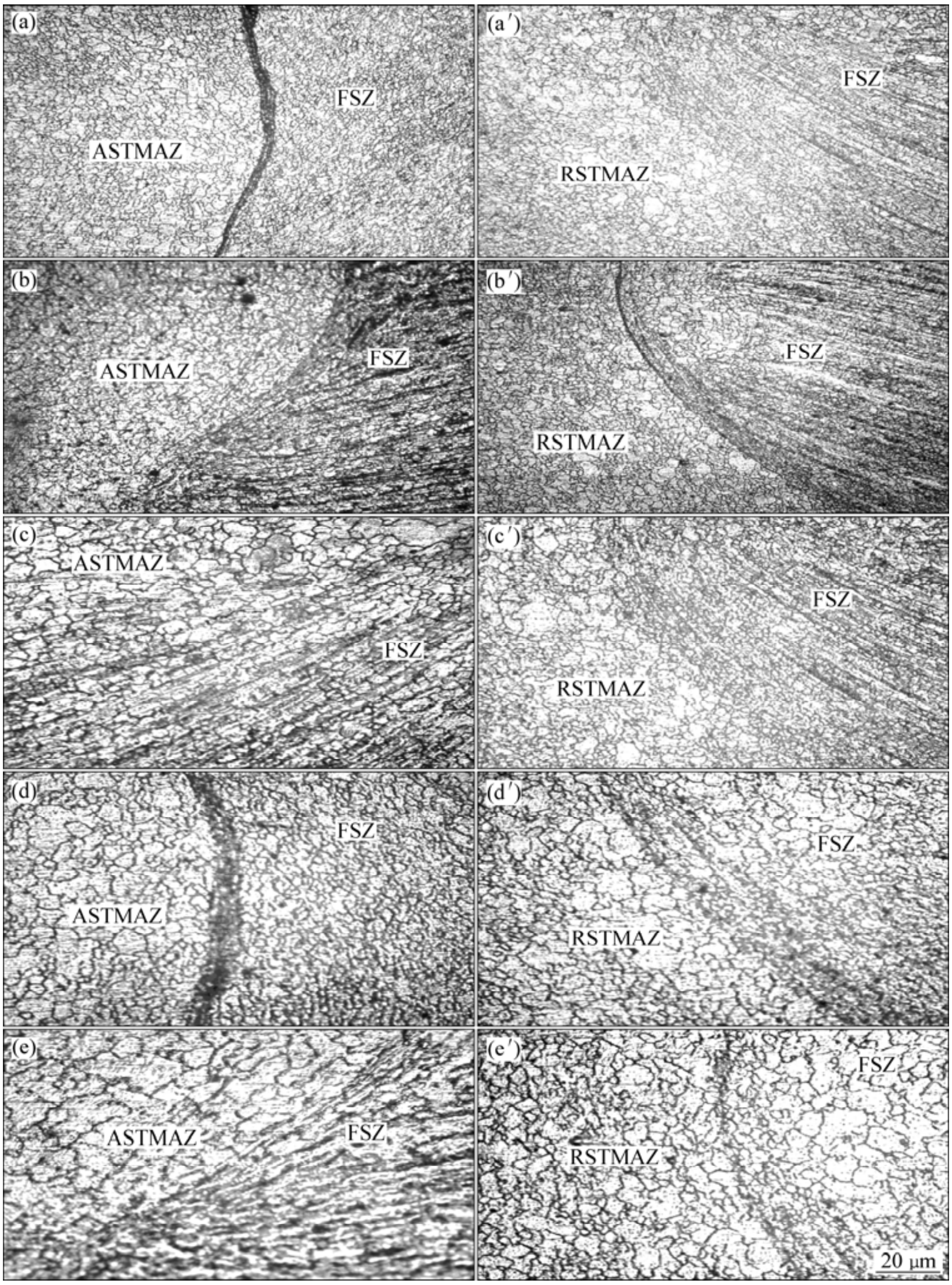

Fig.7 Microstructures of AS and RS (TMAZ) under different axial force: (a), (a′) 3 kN; (b), (b′) 4 kN; (c), (c′) 5 kN; (d), (d′) 6 kN; (e), (e′) 7 kN

used to fabricate the joints. However, minor variation in the shape and size of the dimple is observed and this is mainly due to the difference existing in the stir zone. The fractograph of the joint fabricated under axial force of 5 kN (Fig.9(c)) contains a depression, which is an indication of cup and cone type fracture. This type of failure pattern occurs only when the material undergoes uniform deformation. The uniform deformation in FSW joint is possible only when the stir zone is free from macro level defects. These may be the reasons that the joint fabricated under axial force of 5 kN exhibits superior tensile properties.

4 Discussion

The yield strength and tensile strength of all the joints are lower than those of the base material, irrespective of the axial force used to fabricate the joints. Of the five axial force used to fabricate AZ61A magnesium alloy joints, the joint fabricated under axial force of 5 kN yields superior tensile properties. The above joints show a maximum joint efficiency of 83%

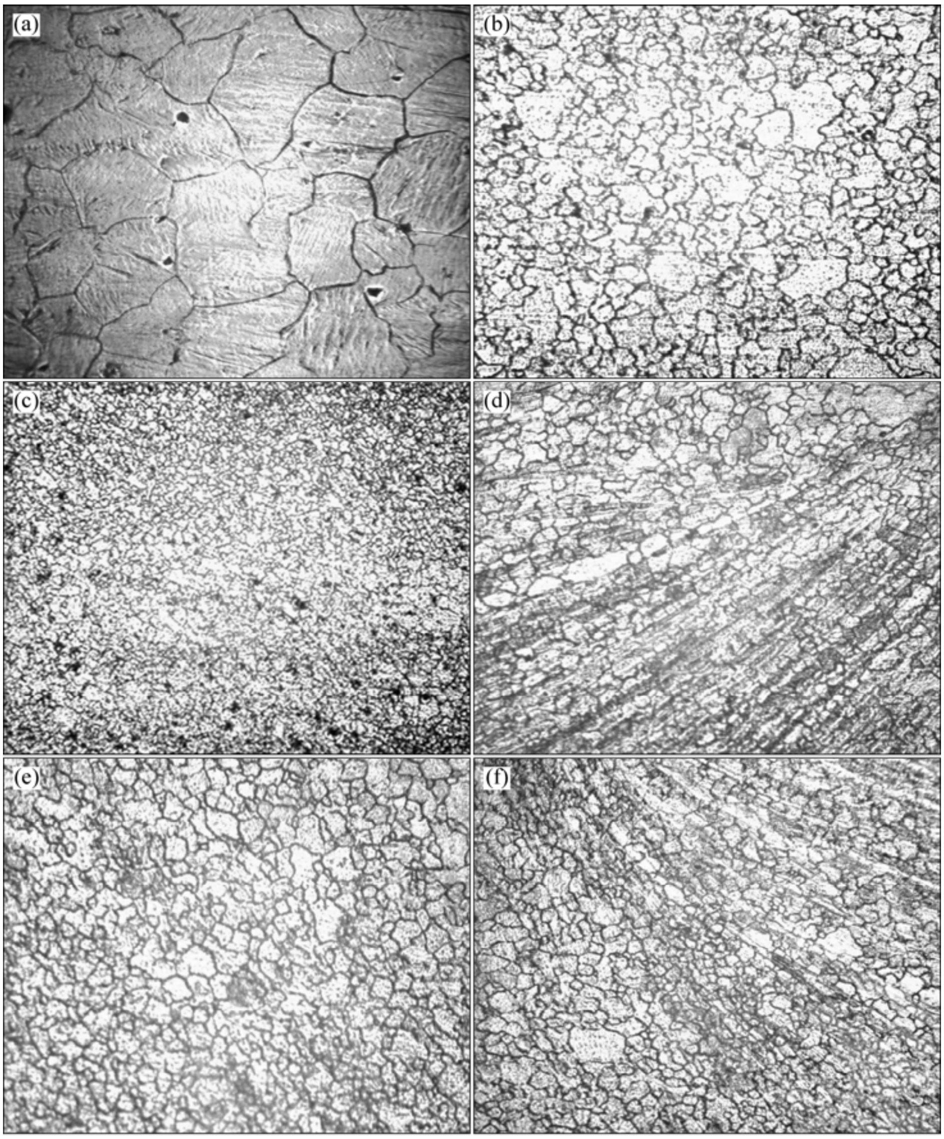

Fig.8 Optical micrographs of defect free joint fabricated at axial force of 5 kN: (a) Base metal; (b) Top side of stir zone; (c) Centre of stir zone; (d) Advancing side of interface; (e) Bottom side of stir zone; (f) Retreating side of interface

compared to other joints. The joints fabricated under axial force lower or higher than this value exhibit comparatively lower tensile properties and the reasons are explained in the following paragraphs.

The initial elongated grains of base metal are transformed into fine equiaxed grains in the weld nugget due to dynamic recrystallization. Under low axial forces, such as 3 and 4 kN, the peak temperature at weld nugget might be very low, and this causes incomplete dynamic recrystallisation. The fragmentation of grains is less due to low axial force, which subsequently results in coarse grains in weld nugget region. If the axial force is too low, the void can propagate all the way to the top surface of the weld nugget where it is exposed to the surrounding environment. This type of defect is known as a lack of surface fill, which is formed when material from the advancing side and the region underneath the shoulder does not consolidate. Unlike the wormhole, the lack of surface fill can be visually detected. Generally, the axial force is too low and a lack of surface fill defect occurs, due to less amount of shoulder contact with the material flow. The temperature during friction stir welding which defines the amount of plasticized metal is greatly dependent on the axial force. Of the five axial forces used to fabricate the joints, the joints fabricated under axial force of 3 and 4 kN exhibit tunnel defect at the middle of the weld zone due to insufficient material flow and lack of stirring at the bottom because of low axial force at the weld nugget.

The increase in axial force increases the heat input to the weld as the frictional force increases. The increased heat input raises the nugget zone temperature and this could lead to static grain growth of dynamically recrystallized grains, which may be the reason for the

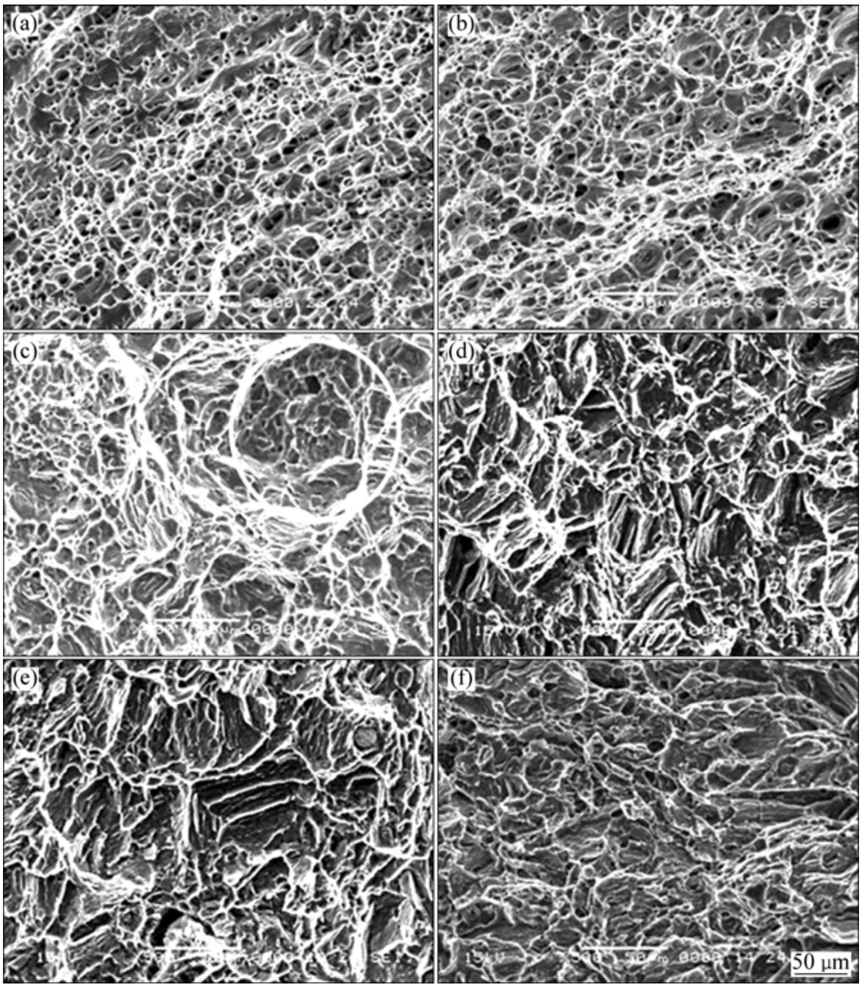

Fig.9 SEM fractographs of unnotched tensile specimens under conditions of different axial force and heat input: (a) 3 kN, 181 J/mm; (b) 4 kN, 242 J/mm; (c) 5 kN, 302 J/mm; (d) 6 kN, 362 J/mm; (e) 7 kN, 422 J/mm; (f) Base metal

formation of finer grains at the weld nugget fabricated under 5 kN axial force due to the sufficient flow of softened material. This may be the reason for higher tensile strength of the joints fabricated under 5 kN axial force compared to the counterparts.

At high axial forces such as 6 and 7 kN, the peak temperature at weld nugget might be very high and this causes turbulent material flow, which subsequently results in defects in the weld nugget region. Moreover, the slow cooling rate of weld nugget after welding also causes grain coarsening. Due to combined effect of these two factors, the tensile strength of the joints fabricated using high axial forces is deteriorated.

5 Conclusions

1) Axial force has significant influences on the formation of defects, grain size and hardness of stir zone and subsequently tensile properties of friction stir welded AZ61A magnesium alloy joints.

2) The joints fabricated under an axial force of 5 kN, rotational speed of 1 200 r/min and welding speed of 90 mm/min exhibit a maximum tensile strength of 224 MPa (83% of the base metal) compared to other joints. The formation of defect free stir zone and finer grains at the stir zone under these welding conditions are responsible for higher hardness and higher tensile strength.

Acknowledgements

The authors are grateful to the Centre for Materials Joining & Research (CEMAJOR), Department of Manufacturing Engineering, Annamalai University, Annamalai Nagar, India for extending their facilities to carry out this investigation. The authors also wish to place their sincere thanks to University Grants Commission (UGC), New Delhi for their financial support rendered through Junior Research Fellowship (JRF) award.

References

[1] MORDIKE B L, EBERT T. Magnesium—Properties, applications, potential [J]. Materials Science and Engineering A, 2001, 302(1): 37−45.

[2] KULEKCI M K. Magnesium and its alloys applications in automotive industry [J]. International Journal of Advanced Manufacturing Technology, 2008, 39(9−10): 851−865.

[3] MUNITZ A, COTLER C, STERN A, KOHN G. Mechanical properties and microstructure of gas tungsten arc welded magnesium AZ91D plates [J]. Materials Science and Engineering A, 2001, 302(1): 68−73.

[4] Magnesium and Magnesium Alloy ASM Specialty Handbook [M]. ASM International, Materials Park, OH, 1999, 3(1): 194−199.

[5] AFRIN N, CHEN D L, CAO X, JAHAZI M. Microstructure and tensile properties of friction stir welded AZ31B magnesium alloy [J]. Materials Science and Engineering A, 2008, 472(1−2): 179−186.

[6] ZHANG H, LIN S B, FENG J C, MA S H L. Defects formation procedure and mathematic model for defect free friction stir welding of magnesium alloy [J]. Materials and Design, 2006, 27(9): 805−809.

[7] LEE W B, YEON Y M, JUNG S B. Joint properties of friction stir welded AZ31 BH24 magnesium alloy [J]. Materials Science and Technology, 2003, 19(6): 785−790.

[8] WANG X H, WANG K S. Microstructure and properties of friction stir butt-welded AZ31 magnesium alloy [J]. Materials Science and Engineering A, 2006, 431(1−2): 114−117.

[9] PAREEK M, POLAR A, RUMICHE F, INDACOCHEA J E. Metallurgical evaluation of AZ31BH24 magnesium alloy friction stir welds [J]. Journal of Material Engineering and Performance, 2007, 16(5): 655−662.

[10] ABBASI GHARACHEH M, KOKABI A H, DANESHI G H, SHALCHI B, SARRAFI R. The influence of the ratio of “rotational speed/traverse speed” (ω/v) on mechanical properties of AZ31 friction stir welds [J]. International Journal of Machine Tool Manufacture, 2006, 46(15): 1983−1987.

[11] ESPARZA J A, DAVIS W C, TRILLO E A, MURR L E. Friction stir welding of magnesium alloy AZ31B [J]. Journal of Material Science Letters, 2002, 21(12): 917−920.

[12] ZHANG H, WU H Q, HUANG J H, Lin S B, WU L. Effect of welding speed on the material flow patterns in friction stir welding of AZ31 magnesium alloy [J]. Rare Metals, 2007, 26(2): 158−162.

[13] CAO X, JAHAZI M. Effect of welding speed on the quality of friction stir welded butt joints of a magnesium alloy [J]. Materials and Design, 2009, 30(6): 2033−2042.

[14] KAZUHIRO N, YOUNG GON K, MASAO U. Friction stir welding of Mg-Al-Zn alloys [J]. Trans JWRI, 2002 , 31(2): 141−146.

[15] PARK S H C, SATO, KOKAWA Y S H. Effect of micro-texture on fracture location in friction stir weld of Mg alloy AZ61 during tensile test [J]. Script Mater, 2003, 49(2): 161−166.

[16] DU Xing-hao, WU Bao-lin. Using friction stir processing to produce ultrafine-grained microstructure in AZ61 magnesium alloy [J]. Trans Nonferrous Met Soc China, 2008, 18: 562−565.

[17] SRINIVASAN P B, ZETTLER R, BLAWERT C, DIETZEL W. Stress corrosion cracking of AZ61 magnesium alloy friction stir weldments in ASTM D1384 solution [J]. Corrosion Engineering, Sci and Technol, 2009, 44(6): 477−480.

[18] KRISHNAN K N. On the formation of onion rings in friction stir welds [J]. Materials Science and Engineering A, 2002, 327(2): 246−251.

[19] OUYANG J H, KOVACEVIC R. Material flow during friction stir welding (FSW) of the same and dissimilar aluminum alloys [J]. Journal of Material Engineering and Performance, 2002, 11(1): 51−63.

[20] BUFFA G, HUA J, SHIVPURI R, FRATINI L. Design of the friction stir welding tool using the continuum based FEM model [J]. Materials Science and Engineering A, 2006, 419(1−2): 381−388.

[21] KUMAR K, KAILAS S V. On the role of axial load and the effect of interface position on the tensile strength of a friction stir welded aluminium alloy [J]. Materials and Design, 2008, 29(4): 791−797.

[22] ELANGOVAN K, BALASUBRAMANIAN V. Influences of tool pin profile and axial force on the formation of friction stir processing zone in AA6061 aluminium alloy [J]. Int J Adv Manuf Tech, 2008, 38(3−4): 285−295.

[23] JAYARAMAN M, SIVASUBRAMANIAN R, BALASUBRAMANIAN V. Effect of process parameters on tensile strength of friction stir welded cast LM6 aluminium alloy joints [J]. J Mater Sci Technol, 2009, 25(5): 655−664.

[24] PADMANABAN G, BALASUBRAMANIAN V. An experimental investigation on friction stir welding of AZ31B magnesium alloy [J]. Int J Adv Manuf Tech, 2009, 49(1−4): 111−121.

[25] ASTM International standard, E 112–04. Standard test methods for determining average grain size [S]. 2006, 3(1): 13−14.

[26] HEURTIER P, JONES M J, DESRAYAUD C, DRIVER J H, MONTHEILLET F, ALLEHAUX D. Mechanical and thermal modelling of friction stir welding [J]. Journal of Material Processing Technology, 2006, 171(3): 348−357.

轴向力对搅拌摩擦焊接 AZ61A 镁合金拉伸性能的影响

A. RAZAL ROSE[1], K. MANISEKAR[2], V. BALASUBRAMANIAN[3]

1. Department of Mechanical Engineering, National engineering College, K.R Nagar−628502, Kovilpatti, Tamil Nadu, India;
2. Centre for Manufacturing Sciences, Department of Mechanical Engineering, National engineering College, K.R Nagar−628502, Kovilpatti, Tamil Nadu, India;
3. Department of Manufacturing Engineering, Annamalai University, Annamalainagar−608002, Chidambaram, Tamil Nadu, India

摘　要：研究轴向力对搅拌摩擦焊接AZ61A镁合金拉伸性能的影响。在3~7 kN范围内选择5个不同大小的轴向力制备接头。测试接头的拉伸性能，并研究其与搅拌区显微组织和硬度的相关性。结果表明，与其他轴向力下的接头相比，轴向力为5 kN时制备的接头具有最好的拉伸性能。搅拌区生成的细晶组织和高硬度是获得高拉伸强度的主要原因。

关键词：镁合金；搅拌摩擦焊；拉伸性能；显微硬度；显微组织

(Edited by FANG Jing-hua)